Supporting Information: NH_3-induced Activation of Hydrophilic Fe-N-C Nanocages for Enhanced Oxygen Reduction Reaction

Bin Wu[a,b], Haibing Meng[c], Dulce M. Morales[d,e], Bo Liu[f], Deniz Wong[g], Christian Schulz[g], Giacomo Zuliani[d], Maddalena Zoli[d], Omeshwari Y. Bisen[d], Samuel Hall[h], Annika Bande[h,i], Zhenbo Wang[f], Marcel Risch[d], Tristan Petit[a,*]

[a] *Young Investigator Group Nanoscale Solid-Liquid Interfaces, Helmholtz-Zentrum Berlin für Materialien und Energie GmbH, Albert-Einstein-Straße 15, 12489 Berlin, Germany*

[b] *Institute of Physics, Humboldt University Berlin, Newton-Straße 15,12489 Berlin, Germany*

[c] *College of Chemistry, Taiyuan University of Technology, 030024 Taiyuan, China*

[d] *Nachwuchsgruppe Gestaltung des Sauerstoffentwicklungsmechanismus, Helmholtz-Zentrum Berlin für Materialien und Energie GmbH, Hahn-Meitner-Platz 1, 14109 Berlin, Germany*

[e] *Engineering and Technology Institute Groningen (ENTEG), University of Groningen, Nijenborgh 3, 9747 AG, Groningen, Netherlands*

[f] *MIIT Key Laboratory of Critical Materials Technology for New Energy Conversion and Storage, School of Chemistry and Chemical Engineering, State Key Laboratory of Space Power-Sources, Harbin Institute of Technology, 150001 Harbin, Heilongjiang, China*

[g] *Department of Dynamics and Transport in Quantum Materials, Helmholtz-Zentrum Berlin für Materialien und Energie GmbH, Albert-Einstein-Straße 15, 12489 Berlin, Germany*

h Theory of Electron Dynamics and Spectroscopy, Helmholtz-Zentrum Berlin für Materialien und Energie GmbH, Berlin, Germany

i Institut für Anorganische Chemie, Leibniz Universität Hannover, Callinstr. 9, D-30167 Hannover

**Corresponding author: tristan.petit@helmholtz-berlin.de*

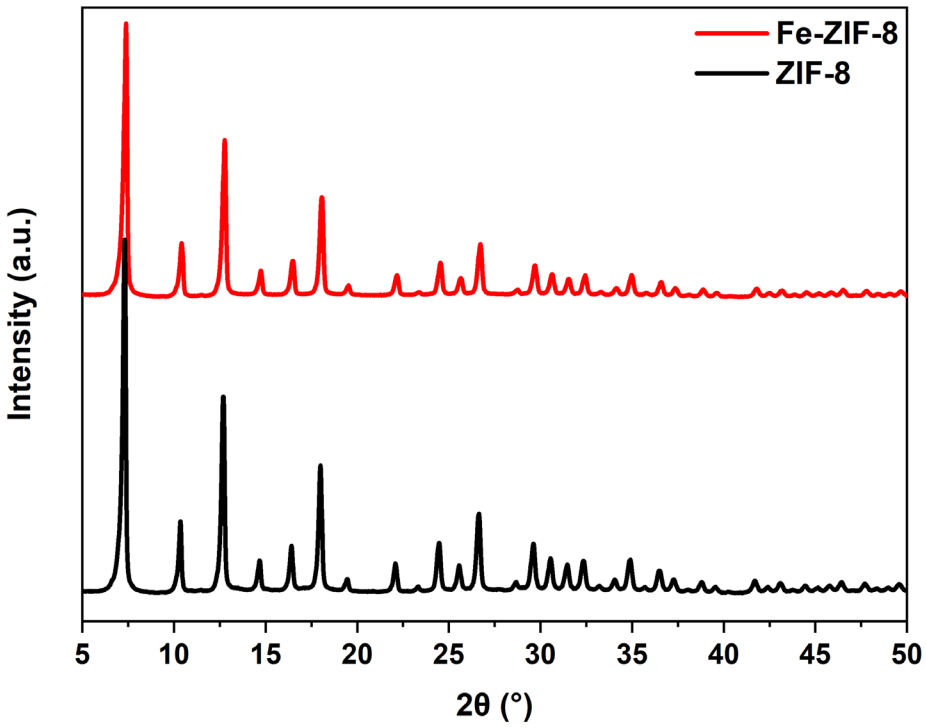

Fig. S1 XRD pattern of ZIF-8 and Fe-ZIF-8.

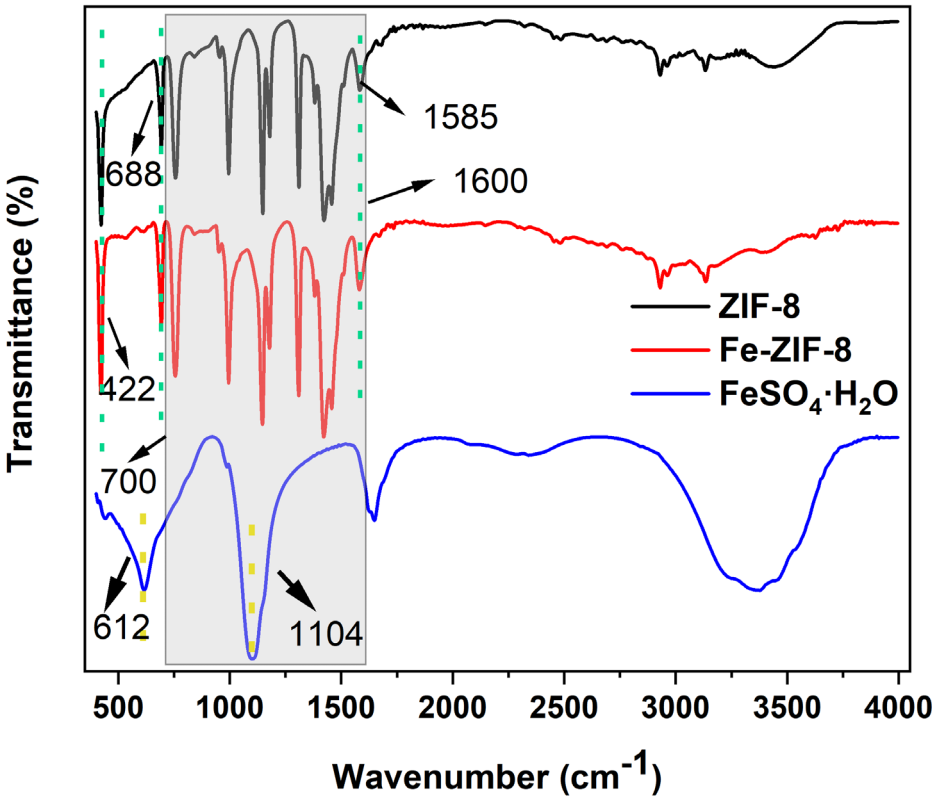

Fig. S2 FTIR spectra of $FeSO_4 \cdot 7H_2O$, ZIF-8 and Fe-ZIF-8.

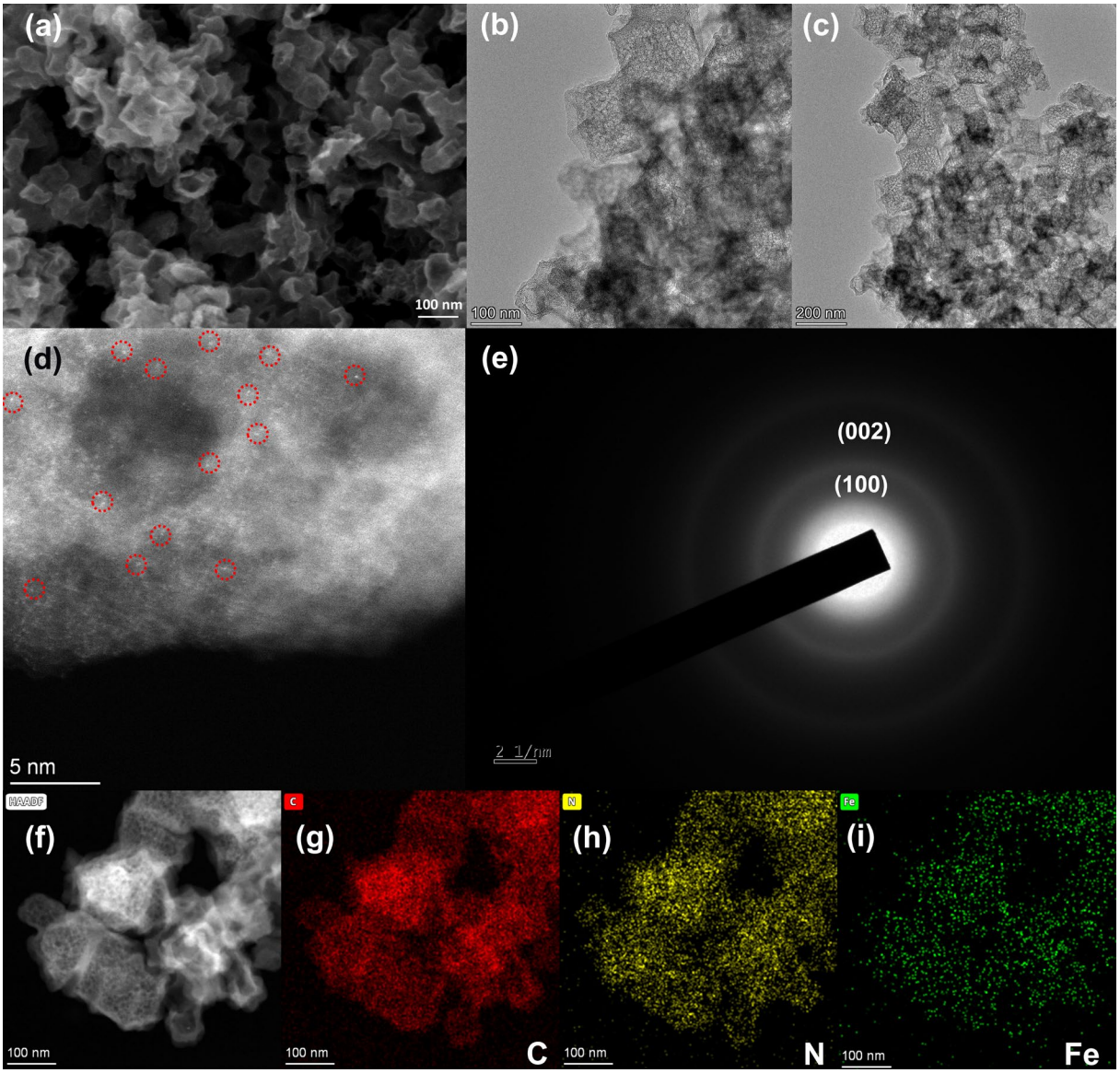

Fig. S3 (a) SEM image of Fe-N-C Ar. (b)-(c) TEM image of Fe-N-C Ar. (d) Aberration-corrected HAADF-STEM image of Fe-N-C Ar. (e) SAED pattern of Fe-N-C Ar. (f)-(i) Elemental mapping analysis of C, N, and Fe of Fe-N-C Ar by HAADF-STEM.

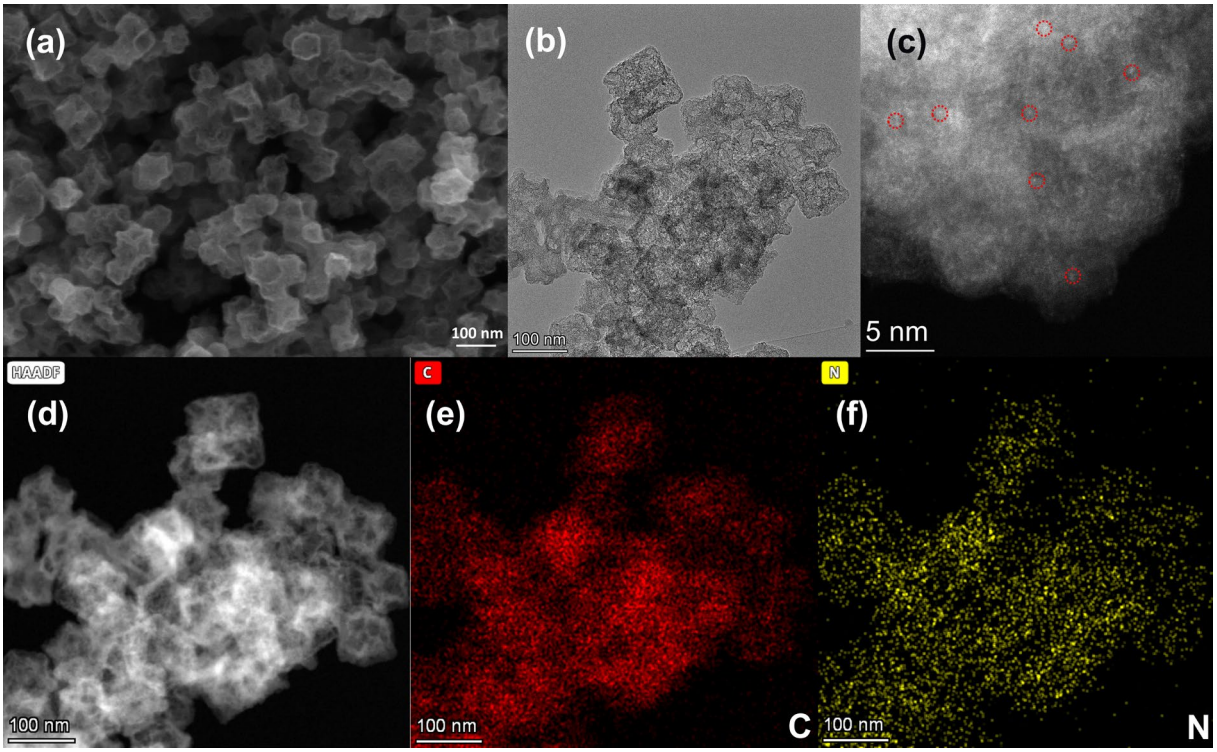

Fig. S4 (a) SEM image of pure NC. (b) TEM image of pure NC. (c) Aberration-corrected HAADF-STEM image of pure NC. (d) SAED pattern of Fe-N-C Ar. (e)-(f) Elemental mapping analysis of C and N of pure NC Ar by HAADF-STEM.

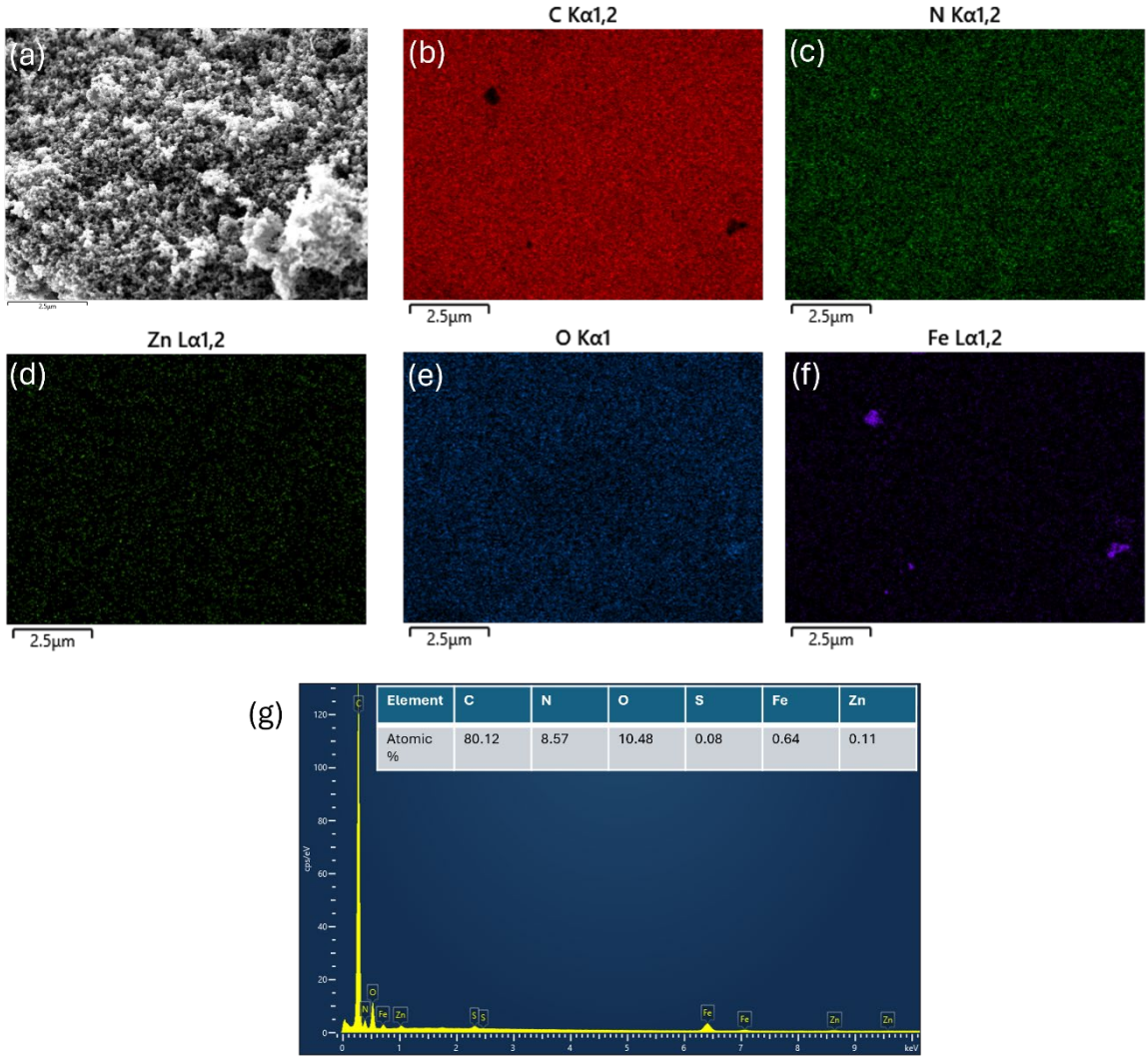

Fig. S5 (a) SEM image of Fe-N-C NH_3. (b-f) Elemental mapping by SEM-EDS. (g) Elemental quantification based on EDS.

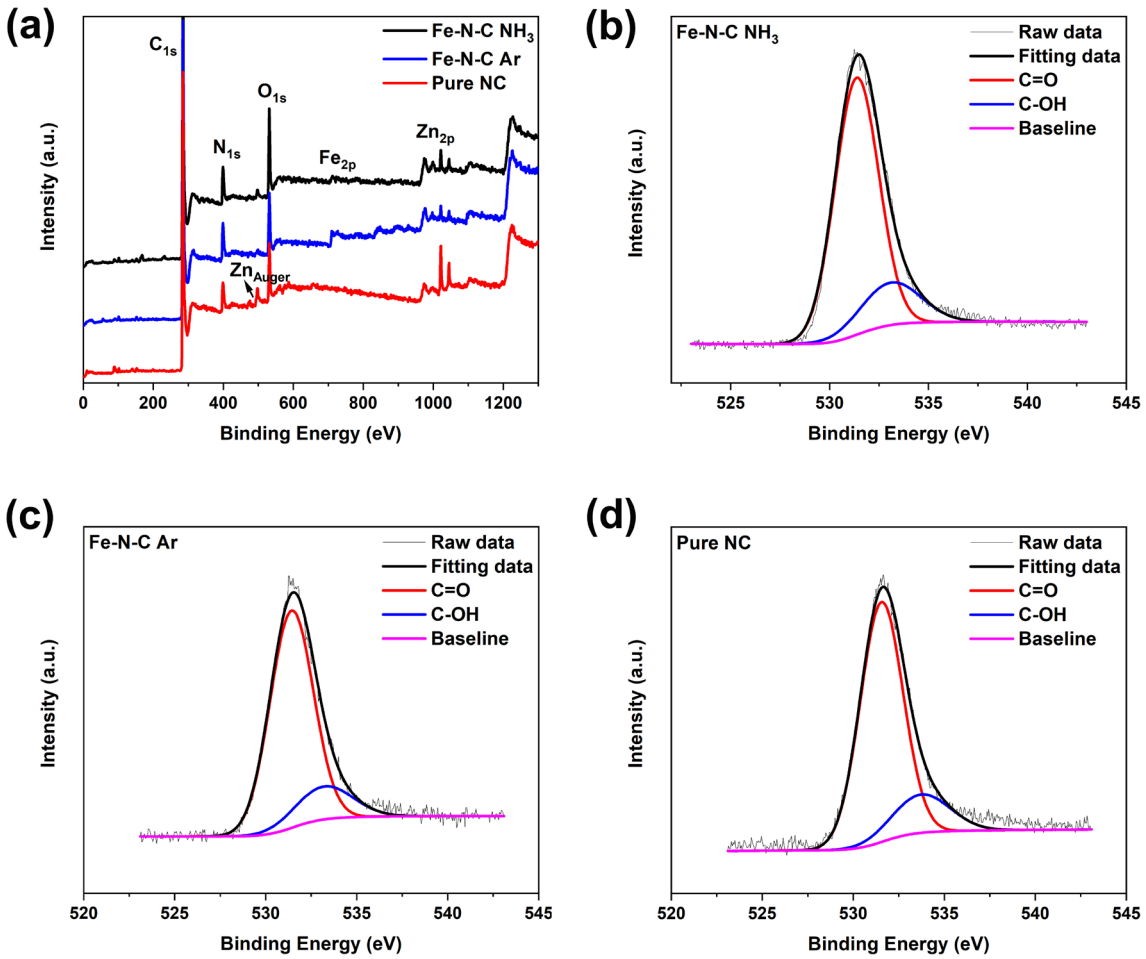

Fig. S6 (a) Overall XPS survey spectra of Fe-N-C NH_3, Fe-N-C Ar and pure NC. (b)-(d) High-resolution O 1s XPS spectra of Fe-N-C NH_3, Fe-N-C Ar and pure NC, respectively.

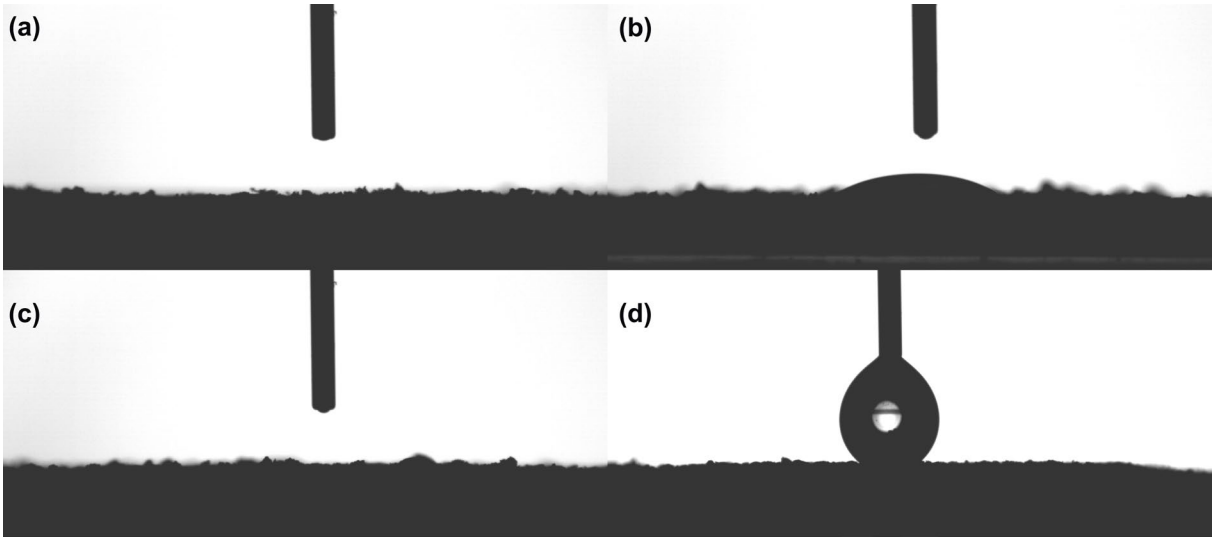

Fig. S7 Contact angle of Fe-N-C NH_3 (a), pure NC (b), Fe-N-C Ar (c) and commercial Pt/C 20% (d).

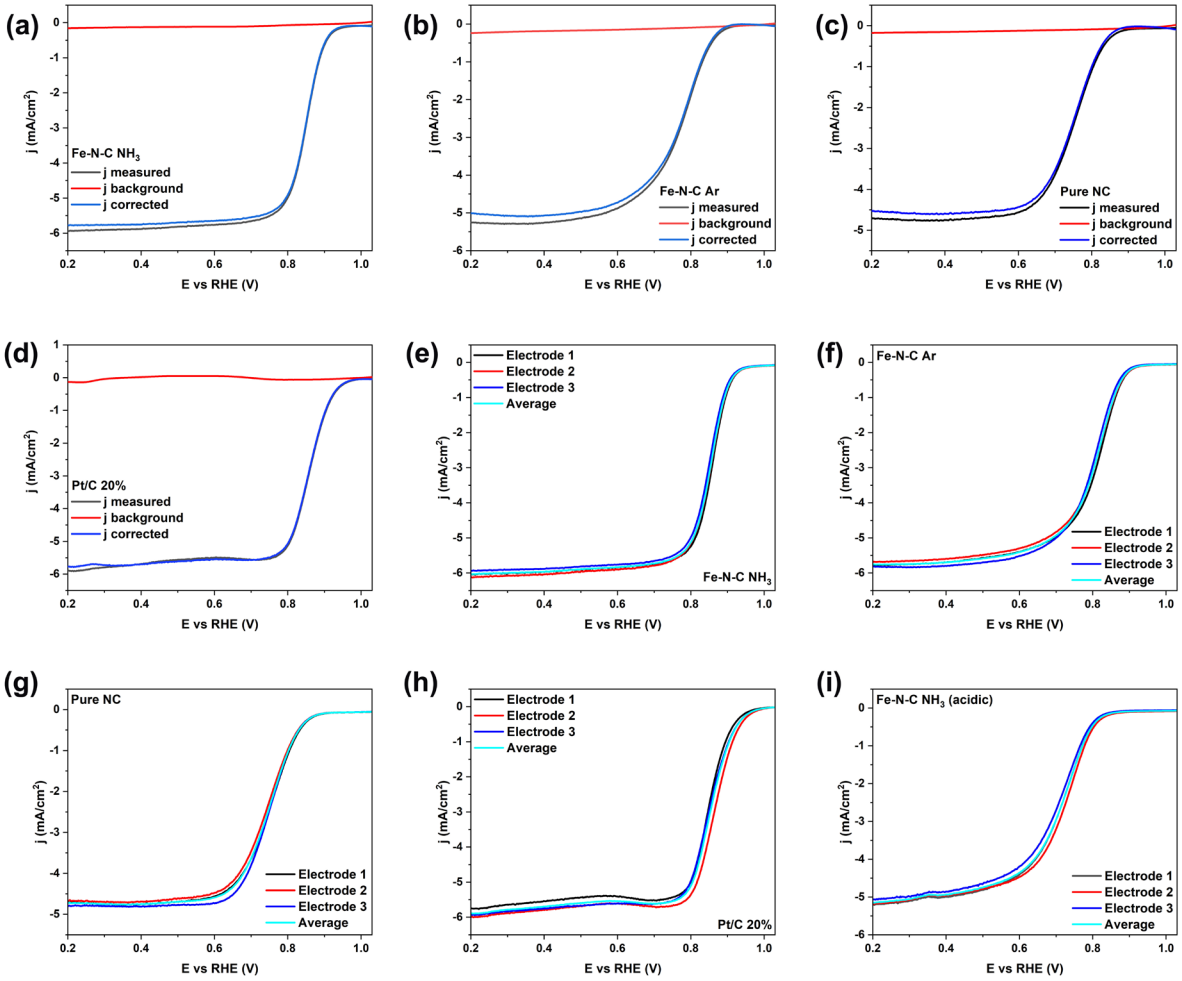

Fig. S8 (a)-(d) ORR voltammograms of Fe-N-C NH_3 (black) recorded in O_2-saturated 0.1 M KOH solution at a scan rate of 5 mV s^{-1} and electrode rotation of 1600 rpm after background-correction (blue) of Fe-N-C NH_3, Fe-N-C Ar, pure NC and Pt/C 20%, respectively; (red) background current recorded in Ar-saturated 0.1 M NaOH electrolyte with the same measuring conditions. (e)-(i) Reproducibility of voltametric measurements collected with Fe-N-C NH_3, Fe-N-C Ar, pure NC, Pt/C 20% and Fe-N-C NH_3 in O_2-saturated 0.1 M KOH and in acidic media (0.5 M H_2SO_4) at a scan rate of 5 mV s^{-1} at 1600 rpm electrode rotation.

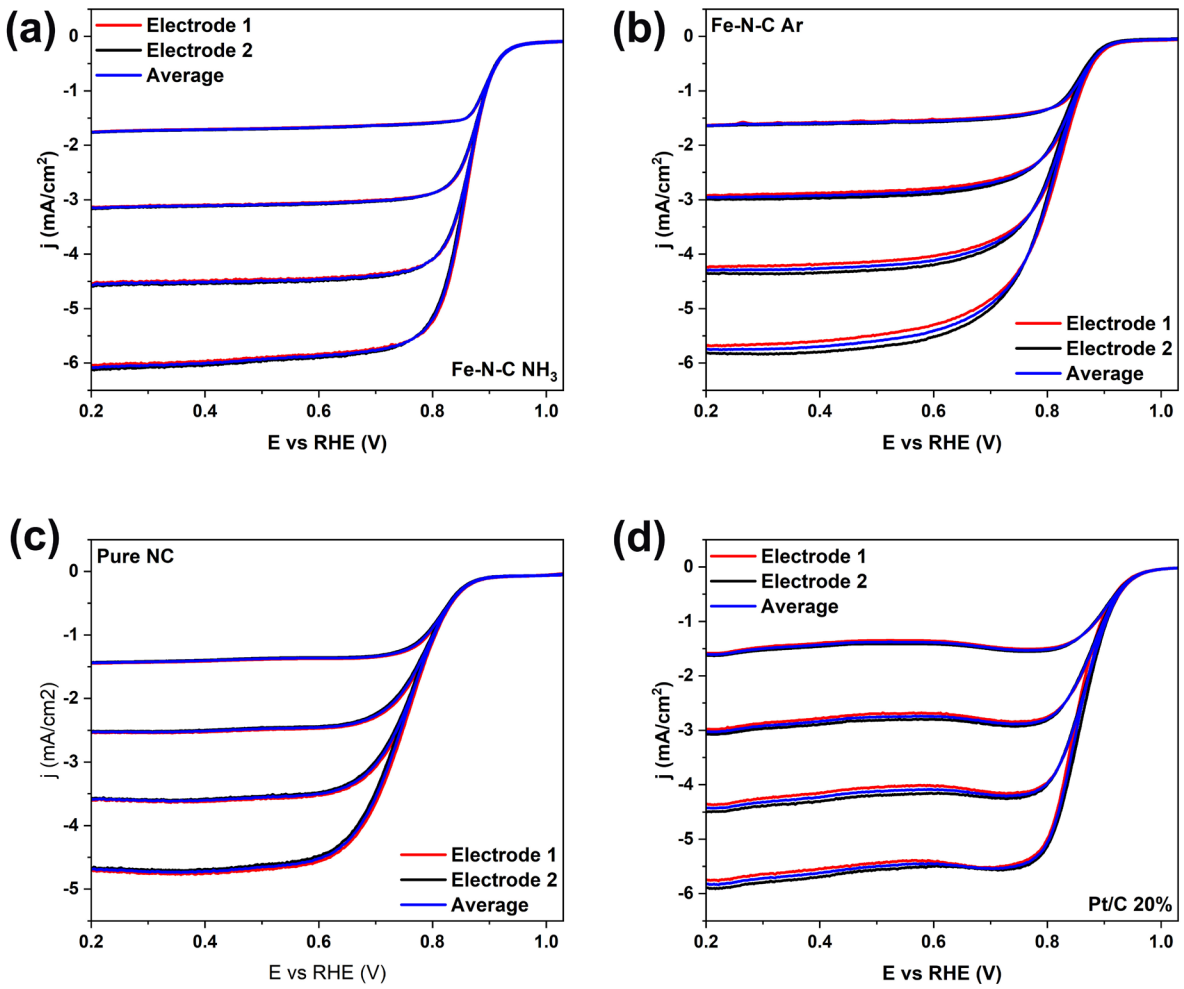

Fig. S9 (a)-(d) Reproducibility of voltametric measurements collected with Fe-N-C NH_3, Fe-N-C Ar, pure NC and Pt/C 20% in O_2-saturated 0.1 M KOH at a scan rate of 5 mV s^{-1} with different electrode rotations.

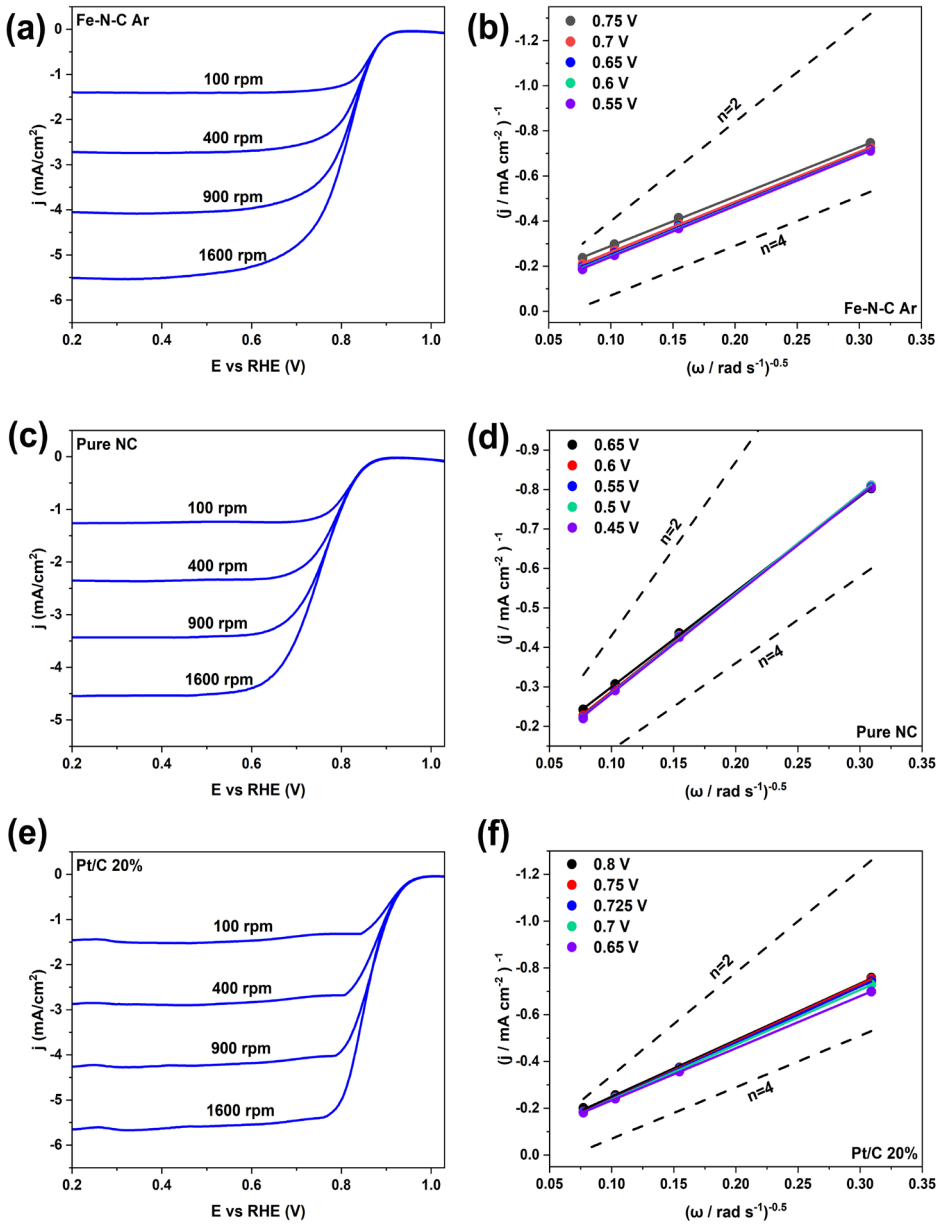

Fig. S10 Background-corrected linear sweep voltammograms recorded at a scan rate of 5 mV s^{-1} with electrode rotation rates of 100, 400, 900 and 1600 rpm of Fe-N-C Ar (a), pure NC (c) and Pt/C 20% (e). The fitted Koutecky-Levich plots at different electrode potentials for the determination of the number of electrons transferred (n) of Fe-N-C Ar (b), pure NC (d) and Pt/C 20% (f); plots corresponding to the theoretical n=2 and n=4 are shown to facilitate visual comparison. All measurements were conducted using an O_2-saturated 0.1 M KOH solution as electrolyte.

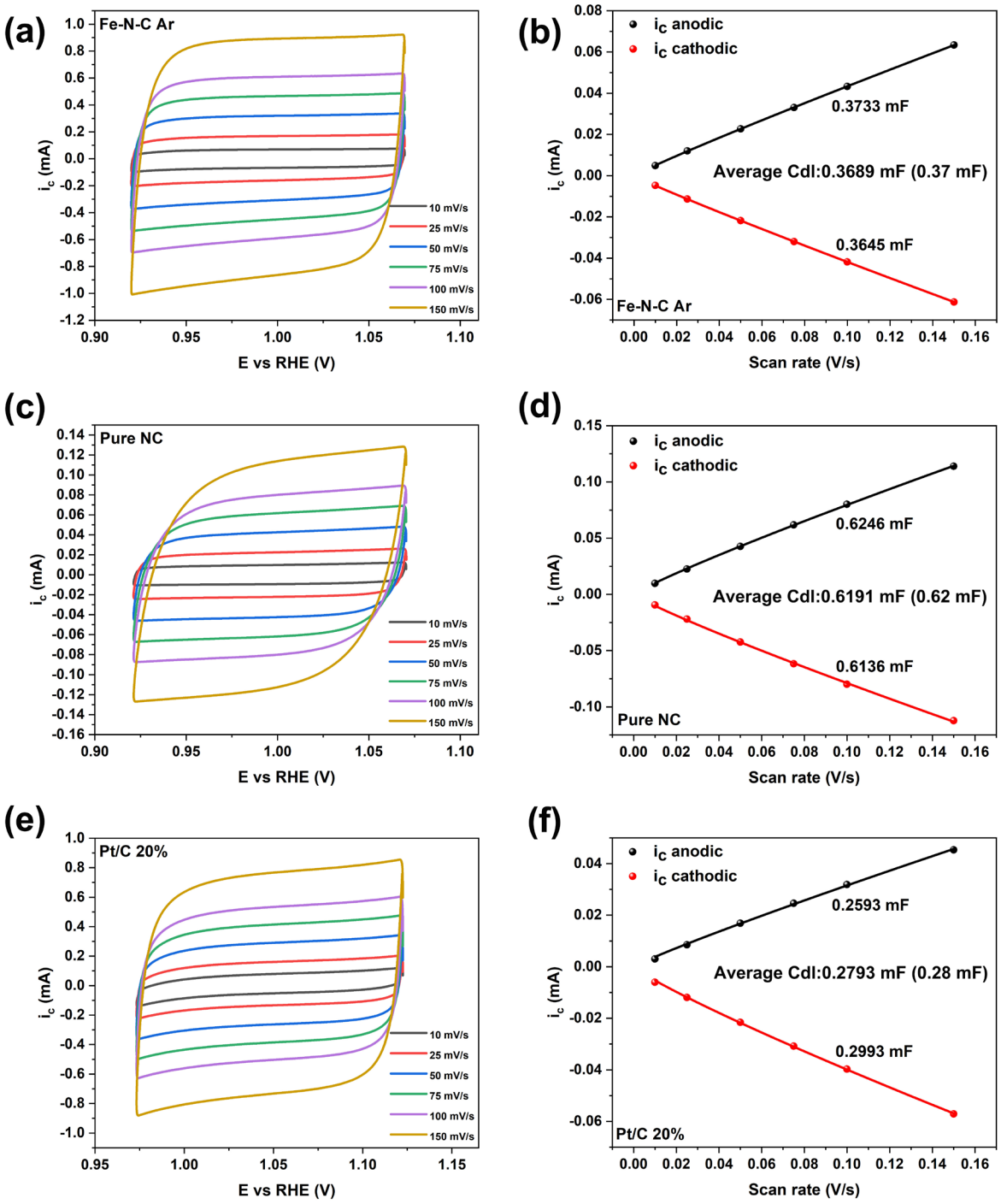

Fig. S11 Cyclic voltammograms recorded at different scan rates from 10 to 150 mV s^{-1} in the potential range of 0.9 to 1.1 V vs RHE for Fe-N-C Ar (a), pure NC (c) and Pt/C 20% (e). The extraction of the Cdl using an allometric function of Fe-N-C Ar (b), pure NC (d) and Pt/C 20% (f). Fit parameters can be found in Table S2.

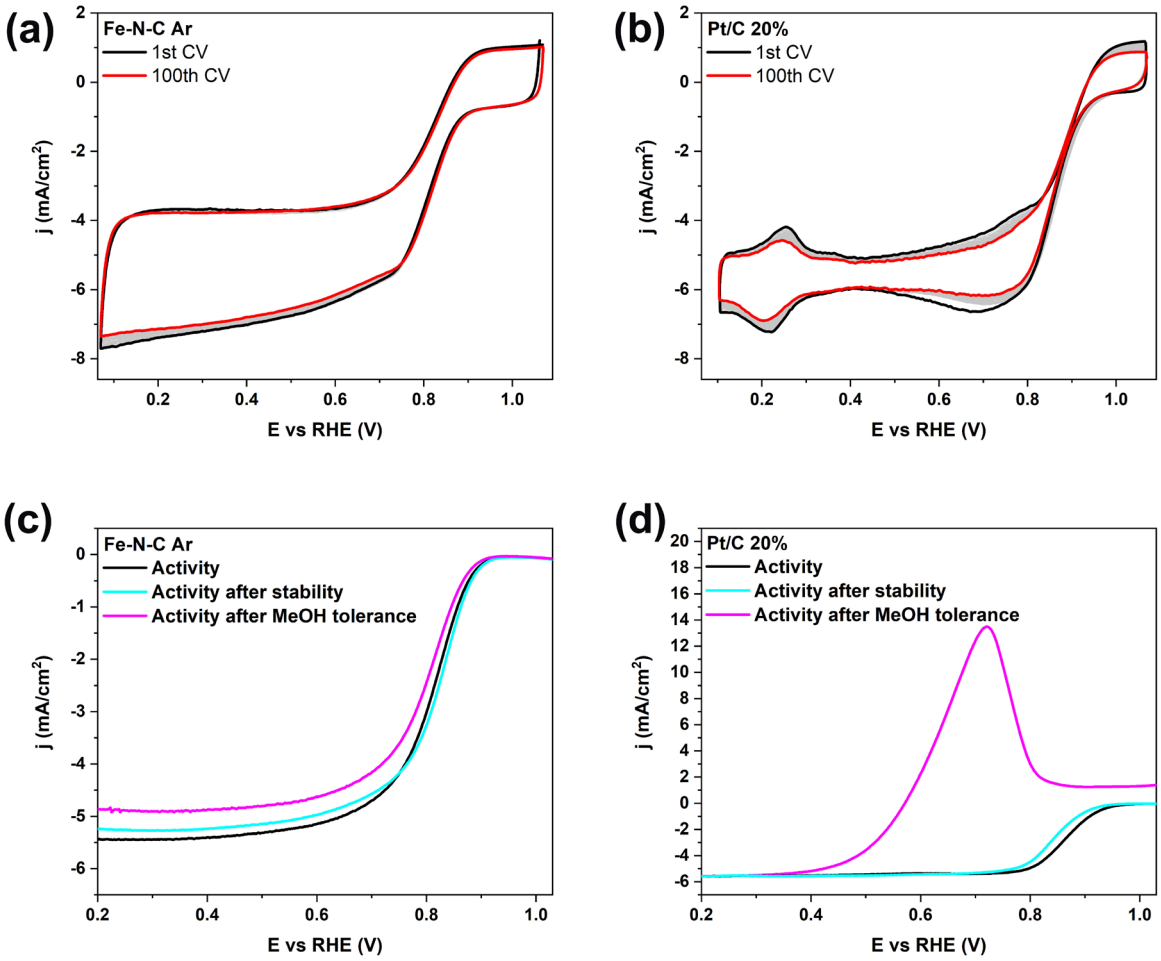

Fig. S12 Stability test recording 100 cyclic voltammograms at scan rate of 50 mV s^{-1} of Fe-N-C Ar (a) and Pt/C 20% (b). ORR activity plots before and after stability test and methanol tolerance in O_2-saturated 0.1 M KOH of Fe-N-C Ar (c) and Pt/C 20% (d).

Table S1 The XPS atomic content of each element for Fe-N-C NH_3, Fe-N-C Ar and pure NC. The error is typically of +- 0.5 at% but Fe atoms are clearly detected.

Materials	Fe at.%	C at.%	N at.%	O at.%
Fe-N-C NH_3	0.26	82.9	7.1	9.7
Fe-N-C Ar	0.7	85.5	7.4	6.5
Pure NC	—	87.5	6.3	6.3

Table S2 XPS Fitting parameters for Fe-N-C NH_3, Fe-N-C Ar and pure NC.

Sample			Fe-N-C NH_3	Fe-N-C Ar	Pure NC
C 1s	C-C	Position (eV)	284.4	284.3	284.3
		FWHM (eV)	1.2	1.1	1.2
		Relative area (%)	43	42	43
	C-N	Position (eV)	285.3	285.1	285.1
		FWHM (eV)	2.7	2.5	2.5
		Relative area (%)	44	44	44
	C-O	Position (eV)	289	288.6	288.4
		FWHM (eV)	3.5	3.7	3.7
		Relative area (%)	14	13	14
N 1s	Pyridinic N	Position (eV)	398.1	398.1	398.1
		FWHM (eV)	1.4	1.5	1.5
		Relative area (%)	35	36	33
	Pyrrolic N	Position (eV)	400.2	400.2	400.4
		FWHM (eV)	2.8	2.9	2.8
		Relative area (%)	56	54	53
	Oxidized N	Position (eV)	403.9	404.3	404.3
		FWHM (eV)	3.7	3.7	3.7
		Relative area (%)	9	11	15
O 1s	C=O	Position (eV)	531.4	531.4	531.5
		FWHM (eV)	2.7	2.8	2.8
		Relative area (%)	82	83	83
	C-OH	Position (eV)	533.1	533.2	533.7
		FWHM (eV)	3.6	3.7	3.7
		Relative area (%)	18	17	18
Fe 2p	Fe $2p_{3/2}$	Position (eV)	710.1	710.4	—
		FWHM (eV)	3.7	5.2	—
		Relative area (%)	29	53	—
	Fe (II) satellite	Position (eV)	714.6	715.4	—
		FWHM (eV)	6.4	2.7	—
		Relative area (%)	27	6	—
	Fe $2p_{1/2}$	Position (eV)	724.2	723.3	—
		FWHM (eV)	9.5	10.7	—
		Relative area (%)	44	41	—

Table S3 Double layer capacitance (Cdl) and corresponding allometric fit parameters of Fe-N-C materials with relevant data sets.

Catalyst	C_{DL}/mFanodic	αanodic	R^2anodic	C_{DL}/mFcathodic	αcathodic	R^2cathodic	C_{DL}/mF average
Fe-N-C NH_3	0.9263	0.9139	0.9992	0.9089	0.9052	0.9996	0.9176
Fe-N-C Ar	0.3733	0.9351	0.9999	0.3645	0.9402	1.0000	0.3689
Pure NC	0.6246	0.8951	0.9999	0.6136	0.8911	0.9995	0.6191
Pt/C 20%	0.2593	0.9151	0.9990	0.2993	0.8751	0.9996	0.2793

Table S4 Performance comparison of some recently reported PGMs-free Fe-based catalysts for ORR.

Catalyst	Electrolyte	Catalyst loading (mg cm^{-2})	Scan rate (mV s^{-1})	E_{-1}*(V vs RHE)	number of electron transfer (n)	Reference
Fe-N-C NH_3	0.1M KOH	0.20	5 mV s^{-1}	0.89	3.98	This work
Fe-N/P-C-700	0.1M KOH	0.60	5 mV s^{-1}	0.91	3.94	[1]
Zn/Fe2–N–C	0.1 M KOH	0.341	5 mV s^{-1}	0.88	3.96	[2]
FePx/Fe-N-C/NPC	0.1M KOH	0.21	10 mV s^{-1}	0.93	3.90	[3]
Fe1-HNC-500-850	0.1M KOH	0.20	5 mV s^{-1}	0.89	NA	[4]
Fe-SAs/NSC	0.1M KOH	0.20	10 mV s^{-1}	0.87	3.96	[5]
Fe/OES	0.1M KOH	0.40	5 mV s^{-1}	0.88	3.90	[6]
Fe-N-C HNSs	0.1M KOH	0.255	5 mV s^{-1}	0.91	3.98	[7]

Supplementary References

1. K. Yuan, D. Lützenkirchen-Hecht, L. Li, L. Shuai, Y. Li, R. Cao, M. Qiu, X. Zhuang, M. K. H. Leung, Y. Chen, and U. Scherf, J. Am. Chem. Soc. **142**, 2404 (2020).

2. J. Xue, Y. Li, and J. Hu, J. Mater. Chem. A **8**, 7145 (2020).

3. Q. Qin, H. Jang, P. Li, B. Yuan, X. Liu, and J. Cho, Advanced Energy Materials **9**, 1803312 (2019).

4. X. Zhang, S. Zhang, Y. Yang, L. Wang, Z. Mu, H. Zhu, X. Zhu, H. Xing, H. Xia, B. Huang, J. Li, S. Guo, and E. Wang, Advanced Materials **32**, 1906905 (2020).

5. J. Zhang, Y. Zhao, C. Chen, Y.-C. Huang, C.-L. Dong, C.-J. Chen, R.-S. Liu, C. Wang, K. Yan, Y. Li, and G. Wang, J. Am. Chem. Soc. **141**, 20118 (2019).

6. C.-C. Hou, L. Zou, L. Sun, K. Zhang, Z. Liu, Y. Li, C. Li, R. Zou, J. Yu, and Q. Xu, Angewandte Chemie International Edition **59**, 7384 (2020).

7. Y. Chen, Z. Li, Y. Zhu, D. Sun, X. Liu, L. Xu, and Y. Tang, Advanced Materials **31**, 1806312 (2019).